JOURNAL OF THERMOPHYSICS AND HEAT TRANSFER
Vol. 10, No. 3, July–September 1996

Mass Spectrometry and Optical Spectroscopy in N_2–CO_2 and N_2–CH_4 Plasma Jets

A. T. Schönemann,* V. Lago,† and M. Dudeck‡
Centre National de la Recherche Scientifique, 92190 Meudon, France

A stationary arcjet at low pressure (0.13 mbar) is used to simulate the properties of the gas flow around a vehicle during entry into the atmosphere of Titan and Mars. For simulation of the Titan atmosphere, a gas mixture of 99% N_2 and 1% CH_4 was used, and for the Martian atmosphere, a gas mixture of 97% CO_2 and 3% N_2 was used. Two different measurement techniques are applied to characterize the plasma: 1) optical emission spectroscopy and 2) mass spectrometry. The composition of the different plasmas, the axial and radial particle distributions of ionized and neutral components, and the vibrational and rotational temperatures were obtained. For the determination of the temperatures a numerical simulation of the molecular band structures of CN was carried out.

Introduction

At the Laboratoire d'Aérothermique, ground test facilities are available for the simulation of the properties of the space environment around a vehicle entering an atmosphere. By means of arcjet generators and a microwave source,[1] rarefied plasma jet flows are obtained. The present investigation was carried out in the plasma wind tunnel SR1 (length 3.4 m, diameter 1 m), where a dc arcjet generator is installed to produce the plasma flows. The arc is obtained between a cathode made of copper with a small zirconium insert at the tip (insert diameter 1.6 mm) and the nozzle throat of a water-cooled copper anode (exit diameter 48 mm). With a vortex-stabilized arc at low currents (50–200 A) and low mass flow rates (0.1–0.3 g/s), stable plasma jets (up to 8 h with air) are obtained. The average specific enthalpy at the end of the arcjet nozzle ranges between 5–22 MJ/kg. Measurements were carried out at 0.13-mbar ambient pressure in the vacuum chamber.

For simulation of entry into the Titan atmosphere a gas mixture of 99% N_2 and 1% CH_4 with a mass flow rate of 0.258–0.005 g/s was chosen. Thus, the amount of CH_4 corresponds to the smallest value expected for the Titan atmosphere.[2] With entry into the Martian atmosphere a mixture of 97% CO_2 and 3% N_2 with a mass flow rate of 0.249–0.0014 g/s was investigated.[3] For all plasmas the arc current was set to 100 A. Thus, an average specific enthalpy at the end of the nozzle exit of 10.9 MJ/kg for the CO_2–plasma and 8.2 MJ/kg for the methane–plasma was reached.

Adding 1% methane to a nitrogen plasma enhances drastically the luminosity of the plasma jet. Unfortunately, within minutes, all water-cooled surfaces inside the vacuum chamber are polluted with a black layer of carbon or carbonic compounds. Since the pollution of the anode leads to an unstable behavior of the arc, the testing time is limited to about 1 h. The quartz window for the optical emission spectroscopy is not water cooled, and there was no significant carbon deposition on it. With a carbon monoxide plasma the testing time is limited by the cathode's lifetime because of relatively fast erosion of the zirconium insert by the hot oxygen and carbon passing along the cathode tip. The cathode has been weighed before and after plasma operation. After 1 h about one-third of the zirconium insert of 0.045 g was lost. The contamination of the plasma jet because of this erosion is estimated to be around 1 ppm. This seems too low to have any influence on the chemical behavior of the plasma. The determination of axial and radial plasma parameters can be obtained by moving the plasma generator along a horizontal and a vertical axis. The system of displacement has a range of 65 cm along the plasma jet axis and a range of 40 cm perpendicular to it. Since the horizontal axis can be displaced itself, distances to the anode of up to 1 m can be reached.

Two different measurement techniques are used: 1) optical emission spectroscopy and 2) mass spectrometry. Both techniques have already been applied to pure nitrogen and air plasmas.[4,5] The experimental setup of the plasma wind tunnel SR1 with both measurement techniques is shown in Fig. 1. The mass spectrometer is fixed to one end of the vacuum chamber opposite the plasma generator while optical emission spectroscopy can be carried out through a small quartz window at one side of the vacuum chamber.

Mass Spectrometer

The mass spectrometer is a Balzers QMG 420 and consists of an electron impact ion source, a quadrupole mass filter, and an electron multiplier. In front of these components an electrostatic lens is installed to guide external ions[6] into the quadrupole for detection. The spectrometer is fixed to one end of the plasma wind tunnel opposite the plasma source. It is operated at a resolution of $m/\Delta m = 1$ at 5% peak height.

The orifice, through which the plasma is sampled, is a 100-μm-diam hole in a 100-μm-thick tungsten foil, that has been fixed on a water-cooled copper plate by a high-temperature soldering technique. This orifice has a small length-to-diameter ratio $L/d = 1$, which is essential for a sampling process of ions and neutrals without any significant disturbance inside the orifice channel. Moreover, the entrance lens of the ion optics is situated just about 4 mm behind the tungsten foil, while the ion source is about 30 mm farther downstream. Thus, short ways and a pressure of 10^{-6} mbar inside the spectrometer assure the unperturbed measurement of both neutrals and ions of the plasma sample. The flat orifice inlet system has proved to give a reliable measurement of the plasma composition in the investigated pressure regime.[7–9] The orifice cooling system limits the closest approach of the plasma generator to 16 cm.

To assure constant conditions of the spectrometer during a measurement inside the plasma jet, a leak dosage system was

Presented as Paper 95-1959 at the AIAA 26th Plasmadynamics and Lasers Conference, San Diego, CA, June 19–22, 1995; received July 21, 1995; revision received Dec. 18, 1995; accepted for publication Jan. 3, 1996.

*Scientist, Laboratoire d'Aérothermique; currently at University of Bern, Physikalisches Institut, Siedlergasse 5, 3012 Bern, Switzerland. Member AIAA.

†Scientist, Laboratoire d'Aérothermique, 4ter Rte des gardes.

‡Professor, 4ter Rte des gardes. Member AIAA.

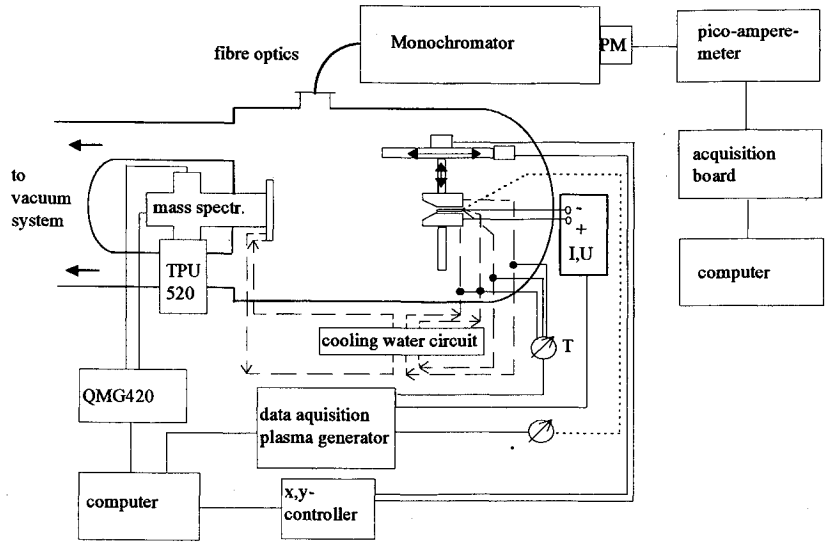

Fig. 1 Scheme of the experimental setup of plasma wind tunnel SR1.

installed. A small amount of a reference gas could be inserted into the ion source, e.g., a reference gas like He at mass number 4 that does not occur into the investigated plasma. This reference signal was observed simultaneously within a measurement of neutral plasma components, a variation of it indicating a significant change of the spectrometer conditions.

The central theme of the plasma beam research at Laboratoire d'Aérothermique is the study of phenomena of space vehicles traversing planetary atmospheres, and we are interested in the plasma around a space vehicle. With the extraction configuration, an orifice in a flat plate perpendicular to the plasma flow, we do not measure the free expanding plasma jet, but the plasma near a wall.

Detection of Neutrals

The detection of neutral plasma components is inevitably disturbed by the residual gas inside the vacuum chamber of SR1 ($p \cong 0.1$ mbar) and the mass spectrometer housing ($p \leq 10^{-6}$ mbar). Considering this, before each test in SR1 a residual gas spectrum was carried out as a reference that could be subtracted from the data gained inside the plasma to yield the real plasma composition. Moreover, the detection of neutral species is influenced by the ion source itself, which produces certain neutrals and ionic fractions of molecules during the ionization process. Therefore, the specific cracking pattern of the plasma molecules has to be a known dependent on the electron energy of the ion source. A calibration was carried out with the neutral gases N_2, O_2, CH_4, CO_2, and H_2O (residual gas), which were fed through the generator without ignition to determine the percentage of the produced fractions N, O, C, CH, OH, CO, CH_2, and CH_3. Molecules as NO and CO could not be calibrated and their cracking patterns were estimated corresponding to the theoretical values (given by Balzers specifications) and to the calibrated data. The measured neutral plasma composition now can be corrected for the known cracking patterns of the main plasma molecules inside the ion source.

Obviously, there is a stagnation point in front of a flat orifice inside a plasma flow. It was shown that the most sensitive parameters to this stagnation point are 1) the detection of ions and 2) the detection of neutral atoms.[9] A small increase of pressure leads to a drastic decrease of the ionic count rates, and a change in the detected ion composition is observed. Thus, high ionic count rates (100,000 counts/s) indicate a small, negligible disturbance of the measured sample by collision processes inside the stagnation point. In fact, while approaching the generator and, to such a degree increasing the

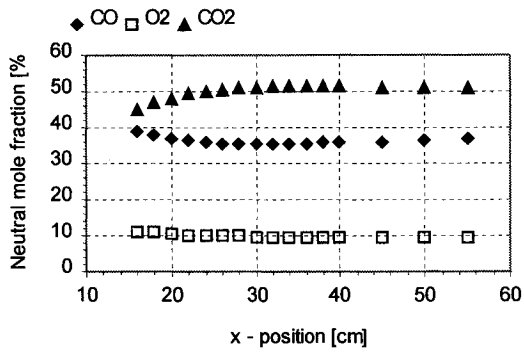

Fig. 2 Axial neutral particle distribution (>10%) of CO_2, CO, and O_2 in a CO_2–N_2 plasma.

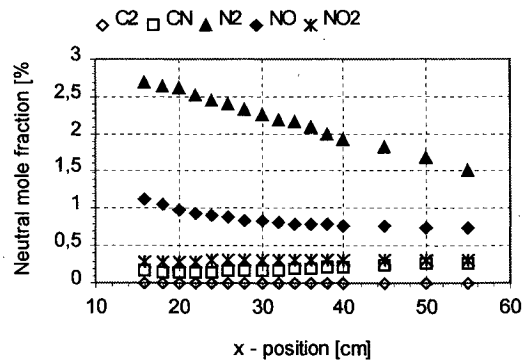

Fig. 3 Axial neutral particle distribution (<10%) of N_2, NO, NO_2, CN, and C_2 in a CO_2–N_2 plasma.

stagnation pressure, the measured total count rate of ions was drastically increasing during the test.

The measurement error, i.e., standard derivation of data after several tests in the plasma wind tunnel SR1, was found to be about 10% for species that need no ion source correction, and 15% for all others. Since it did not account for any mass discrimination of the quadrupole or the electron multiplier, the total error for all of the following results adds up to about 20–25%.

The neutral mole fractions were found by summing up the intensity of all neutrals of a plasma after correcting for each distribution and calculating each particle mole fraction relative to this total intensity. Figures 2 and 3 show the axial distribution of neutral particles in a CO_2–N_2 plasma. The main

component is about 50% CO_2, but it decreases close to the generator. A comparison of the data with that of a pure CO_2 plasma showed that the amount of particles at mass number 14 (atomic nitrogen) corresponds directly to the increase at mass number 28 (molecules CO and N_2) when adding N_2 to the plasma. The amount of N_2 within the gas mixture could be recalculated because of the cracking pattern of N_2 in the ion source. The distribution of neutrals is continued by CO, O_2, N_2, NO, NO_2, CN, and a small amount of C_2 (<0.1%). Like CO_2, the species C_2, CN, and NO_2 show a decrease when approaching the generator, while N_2, CO, NO, and O_2 are increasing. Radial distributions show no significant changes in composition within a jet diameter of 20 cm, except for N_2, which is found mainly in the center of the jet.

Obviously, the CO_2 is dissociated by the arc forming the molecules CO and O_2. Close to the anode where the temperatures are higher these reactions are preferred. No atomic species could be found up to a distance of 16 cm. The main reaction inside the plasma jet is the dissociation of CO_2 to CO and O, and the following associative dissociation reaction of CO_2 with O to CO and O_2. There is only a small amount of C_2 and CN formed, whereas no neutral atomic particles could be found up to a distance of 16 cm. The main reaction inside the plasma jet is the dissociation reaction of CO_2 to CO and O, and the following associative dissociation reaction of CO_2 with O to CO and O_2. These reactions were proposed also as main reactions by the reaction scheme of Park.[3] There is only a small amount of C_2 and CN formed in the jet.

Figures 4 and 5 depict the axial distribution of neutrals in the N_2–CH_4 plasma. Since a lot of molecular combinations of C, H, and N exist, nearly all possible masses up to mass number 52 have been observed in the plasma jet. Unfortunately, a lot of these molecules occur at the same mass number and cannot be separated with the mass spectrometer. Therefore, the species are not named in the figures, but the mass numbers (atomic mass unit) are mentioned. The mass numbers are related to the most probable compounds in the following paragraph.

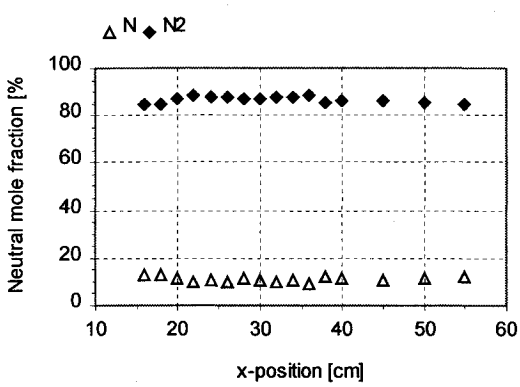

Fig. 4 Axial neutral particle distribution (>1%) of N_2 (28 amu) and N (14 amu) in an N_2–CH_4 plasma.

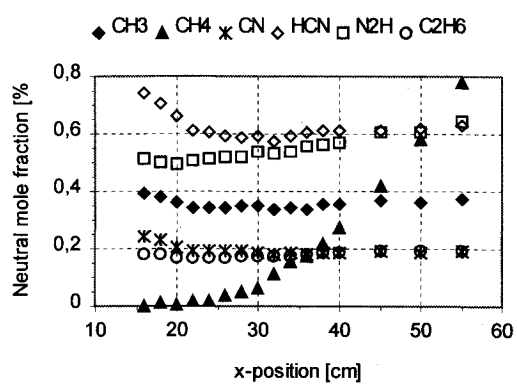

Fig. 5 Axial neutral particle distribution (<1%) in an N_2–CH_4 plasma.

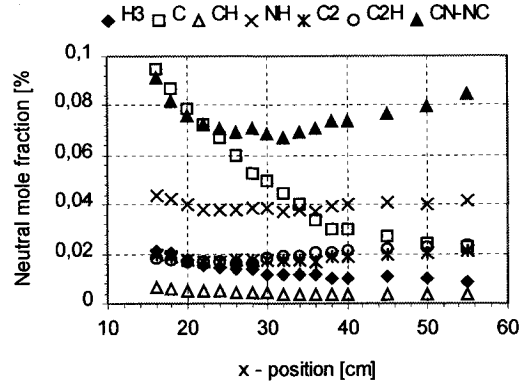

Fig. 6 Axial neutral particle distribution (<0.1%) in an N_2–CH_4 plasma.

The main component in the methane plasma is N_2 (28 amu) with about 80–90%, followed by atomic nitrogen (14 amu) with about 10% (Fig. 4). A small amount of CH_2 has to be assumed within the percentage of N. Other neutrals that were found in the plasma jet all show a mole fraction of $\leq$1%. Those are (mass numbers in parentheses): H_3 (3), C (12), CH (13), NH (15), CH_3 (15), CH_4 (16), C_2 (24), C_2H (25), CN/C_2H_2 (26), HCN/C_2H_3 (27), N_2H/C_2H_5 (29), C_2H_6 (30), and a particle at mass 52 amu, which was assumed to be the molecule cyanogen,[2] namely NCCN (Figs. 5 and 6).

The distinction of NH and CH_3 was made by a comparison of the signal at mass number 15 in a nitrogen–methane mixture, and by slowly lowering the percentage of the methane to zero, a pure nitrogen plasma. The peak intensity at mass number 15 is directly proportional to the amount of methane in the gas mixture. The main part of the signal can be considered to be CH_3 (Fig. 5, $\approx$0.4%).

The molecule H_2 was also detected during a test, but it is difficult to give a quantitative analysis of its signal. The mass spectrometer has a poor resolution for low masses. Also, the peak intensity of H_2 is lower under plasma conditions than during a residual gas measurement. A mass spectrum corrected for residual gas would give a negative signal for this molecule. Finally, the signal decreases when approaching the generator. This seems to imply that molecular hydrogen, as for light mass numbers, is measured with a lower resolution in comparison with the higher mass numbers, and is therefore, not presented in a figure. The peak intensity of molecular hydrogen is drastically lowered inside the plasma compared with the residual gas measurement. Thus, a residual gas correction will yield a highly negative value. Additionally, the amount of H_2 decreases when approaching the generator. As a result, it can be said that molecular hydrogen is strongly consumed by the plasma. There are some possible reactions for the loss of molecular hydrogen, but the presented data give no explanations. Because of the complications connected with the interpretation of this signal, we didn't present it in the figures. Atomic hydrogen was not investigated during the test.

Nearly all neutral components show the same behavior as N_2 and N, a nearly constant distribution, except for a small increase close to the generator. There are four remarkably different slopes: C, CH_4, H_3, and NCCN. CH_4 is steeply decreasing over the whole measurement range and vanishes close to the generator. The species C and H_3 are steeply increasing over the axial range while NCCN rises steeply like C from a position of 30 cm to the anode. Thus, methane is nearly totally dissociated by the arc forming mainly atomic carbon. Again, as for the CO_2 plasma, the production of C_2 is low, <0.1%. The total amount of CN in the methane is higher, but if all molecules containing CN are summed up (CN, HCN, and NCCN) it is still less than 1%. There is a great variety of

species found within our plasma (see the following paragraph for ions), which are not included in the actual chemistry model of Nelson[2] for Titan. N_2, N, and CH_4 compare quite well, while others, e.g., CN, are found only with low percentages or are not present at all (e.g., H^+).

Detection of Ions

For the detection of ions the ion source is switched off and the voltages of the electrostatic entrance lens are optimized for maximum transmission of external ions. The sampling of ions is disturbed mainly by the plasma sheath in front of the flat orifice and by the collisions with other species because of the stagnation point. While the plasma sheath influences the ion energies that are not measured at all, for the given conditions, low ambient pressure in the vacuum chamber and an orifice with $L/d = 1$, the effect of the composition changes in the stagnation point is negligibly small. Thus, no correction was applied to the data gained inside the plasma jet. The ion mole fractions are determined by summing up the intensity of all plasma ions and calculating the mole fraction of each ion relative to this total intensity.

Figures 7 and 8 depict the ion distribution in the CO_2-N_2 plasma. Main ionic species in the plasma jet are O_2^+, CO_2^+, and NO^+ with a contrary slope. Atomic species are also found, O^+ with about 1%, while C^+ with 0.2% close to the anode. N^+ can be observed at a distance of 16 cm with a percentage of less than 0.1% (not shown in Fig. 8). There are some molecular ions that occur because of charge transfer and associative charge transfer reactions of plasma species with residual gas particles like H_2O^+, CO_2H^+, and COH^+, the latter are typical products of plasmas where some hydrogen is present. Some of the ions that are strongly present in our experiments' most intense ions are not considered by the Park[3] model, as there are CO_2^+, O_2^+, NO_2^+, and CN^+ (<0.05%). This may arise because of the different pressure range used here.

In Figs. 9 and 10 the ion distribution in the methane plasma is given. Within these two figures only the main ionic components are shown. Other species that occur at higher mass

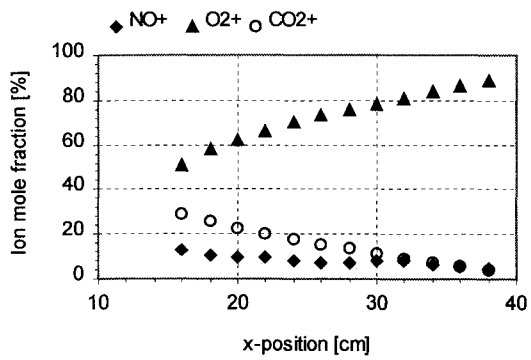

Fig. 7 Axial ion distribution in a CO_2-N_2 plasma (>5%).

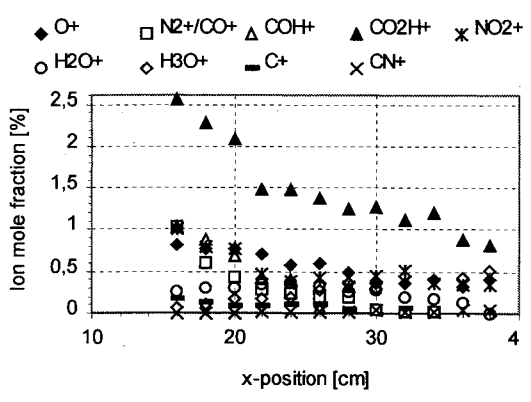

Fig. 8 Axial ion distribution in a CO_2-N_2 plasma (<5%).

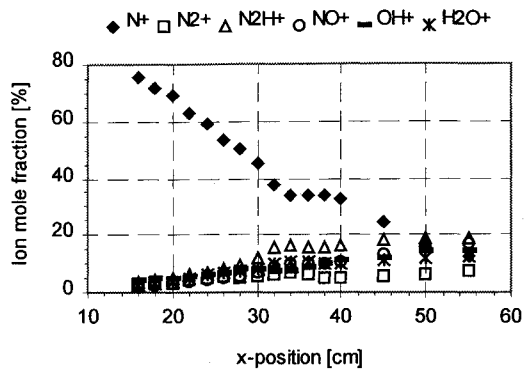

Fig. 9 Axial ion distribution in an N_2-CH_4 plasma (>10%).

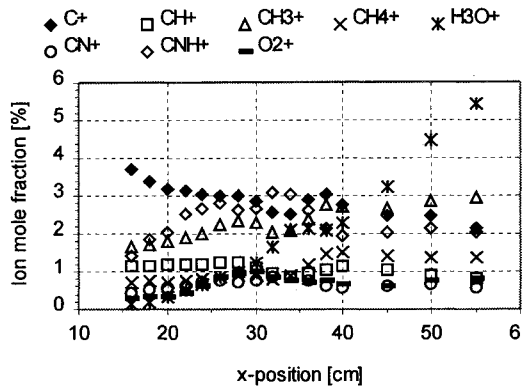

Fig. 10 Axial ion distribution in an N_2-CH_4 plasma (<10%).

numbers (38–45 amu) have been observed, but with percentages smaller than 0.1%, and they are not presented here. Ions present in the plasma jet are (mass numbers in parentheses): C^+ (12), CH^+ (13), N^+ (14), CHO^+/NH (15), CH_4^+/O (16), OH^+ (17), H_2O^+ (18), H_3O^+ (19), $CN^+/C_2H_2^+$ (26), $HCN^+/C_2H_3^+$ (27), N_2^+ (28), $N_2H^+/C_2H_5^+$ (29), $NO^+/C_2H_6^+$ (30), and O_2^+ (32). The most probable ion was mentioned first in the previous list.

The most important ion is N^+ that rises up to 80% close to the anode. All other ions, except for C^+, show a descending slope when approaching the generator. Most ions, especially those containing oxygen like H_2O^+ or NO^+, are produced by charge exchange reactions of the main plasma component N^+ with residual gas particles reducing the amount of N^+ to the same order as for these secondary ions. Even close to the anode no atomic or molecular hydrogen was detected.

Optical Emission Spectroscopy

Since arcjets are luminous, some of their physical parameters can be determined by observing the emitted light with means of optical emission spectroscopy (OES), which is a nonintrusive diagnostic tool. Rotational and vibrational spectra can be deduced in low-pressure plasma jets from OES in the visible and the near uv range. Therefore, a high resolution is needed to resolve the rotational lines.

The experimental setup was also presented in Fig. 1. A fiber optic system is used to image the plasma light onto the entry slit of the monochromator. The monochromator has a focal length of 1500 mm, is fitted with a 1200 lines/mm grating, and has a spectral range between 227–700 nm.

The dispersed light is detected with a Hamamatsu 928 photomultiplier while its output is sent to a picoamperemeter. Afterwards, the analogous output is recorded with an acquisition board linked to a computer.

Vibrational and Rotational Spectra

Different vibrational spectra are recorded for the nitrogen–methane plasma. The violet system of the CN radical is observed, which is because of the transition

$$CN(B^2\Sigma, v') \rightarrow CN(X^2\Sigma, v'')$$

Two sequences are clearly visible under our plasma conditions: the $\Delta v = 0$ (Fig. 11), whose bandheads are (0–0) at 388.34 nm, (1–1) at 387.14 nm, (2–2) at 386.19 nm and the (3–3) at 385.47 nm, and the $\Delta v = -1$ (Fig. 12). Here the (0–1) bandhead at 421.6 nm up to the (5–6) bandhead at 415.24 nm is observable. Two other molecular band structures have been observed: the transition of NH (Fig. 13),

$$NH(A^3\Pi, v') \rightarrow NH(X^3\Sigma, v'')$$

whose bandhead is at 336.0 nm, and the transition of CH with a bandhead at 431.5 nm.

In the CO_2–N_2 plasma, which is as luminous as the N_2–CH_4 plasma, a lot of emission can be found, but the excitation levels are too low for most of the molecules to identify the species exactly. Thus, only the violet system of CN could be recognized (Fig. 14).

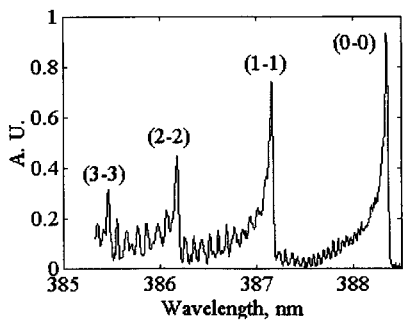

Fig. 11 $\Delta v = 0$ band structure of CN measured at the nozzle exit in an N_2–CH_4 plasma.

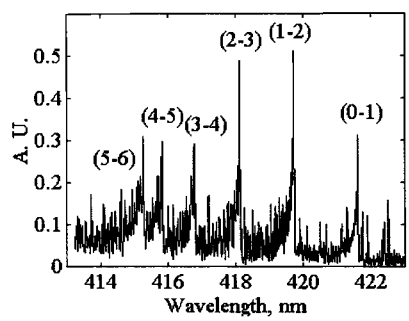

Fig. 12. $\Delta v = -1$ band structure of CN measured at the nozzle exit in an N_2–CH_4 plasma.

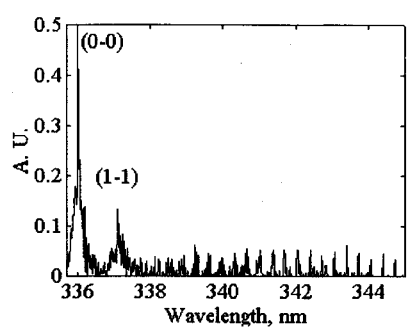

Fig. 13 $\Delta v = 0$ band structure of NH measured at the nozzle exit in an N_2–CH_4 plasma.

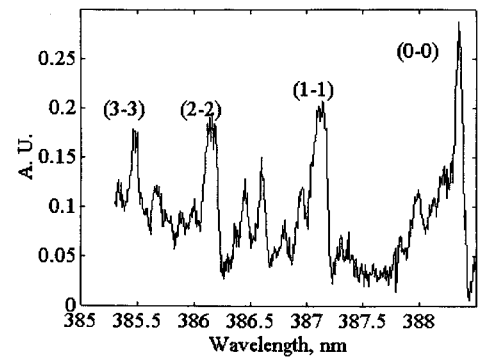

Fig. 14 $\Delta v = 0$ band structure of CN measured at the nozzle exit in a CO_2–N_2 plasma.

The purpose of the study is to deduce the rotational and the vibrational temperatures from the experimental spectra at several positions in the plasma jet using a comparison with calculated spectra.[10] Unfortunately, the Boltzmann plot method cannot be applied to determine the rotational temperature from the (0–0) band of CN. As a matter of fact, it is very difficult to measure the lines intensities because of (Ref. 11) the overlapping of the P and R branches for the same band with $N_p = N_r + 57$ and the overlapping of the P branches arising from itself with $N'_p = 56 - N_p$, N'_p ranging between 1–55.

To overcome this difficulty, for the determination of the rotational and vibrational temperature, a simulation of the $\Delta v = 0$ and the $\Delta v = -1$ band of CN was carried out.

Calculated Spectra

Both spectra of CN were calculated using assumptions concerning the two electronic states $B^2\Sigma^+$ and $X^2\Sigma^+$. Each electronic state obeys to the case (b) of the Hund's selection rules. The spectral intensity is proportional to the density of the upper level. We consider that the radiating upper level is populated by electron collisions from the ground state. In our case, the local thermal equilibrium (LTE) cannot be assumed because the electron density is too low for that ($Ne \approx 10^8$–10^{12} cm^{-3}). This assumption can be assisted with the criterium proposed by Mcwhitrter,[12] which gives the inequality about the electron density necessary to satisfy the LTE model plasma:

$$N_e \geq 1.6 \times 10^{12} T_e^{1/2} \chi(p, q)^3 \text{ cm}^{-3}$$

where T_e is the electron temperature in Kelvin and $\chi(p, q)$ is the excitation potential of level p from level q in electron volts. For the transition $CN(B^2\Sigma, v') \rightarrow CN(X^2\Sigma, v'')$, the excitation potential is 18 eV, taking an electron temperature between 1000–10,000 K, the right side of the inequality ranges between 2.9×10^{17} and 9.3×10^{17} cm^{-3}. This inequality is not verified, and the LTE model cannot be applied to describe our plasma jets. The estimation of the population of the upper level assumes that the shape of the cross section for excitation by electron collision is the same for the different vibrational levels. This cross section is calculated from the global cross section with a weighting factor corresponding to the Frank–Condon factor transitions, and the vibrational temperature is the temperature of the species of the ground state $CN(X^2\Sigma)$ for the CN spectra. Since the neutral density is low, no quenching of excited levels has to be considered. The radiate transition probabilities are given in Ref. 13.

The entry parameters for the calculation of the simulated spectra are 1) the range of wavelength, 2) the monochromator's apparatus function, and 3) the rotational and vibrational temperatures.

Since the rotational terms for $J = 60$ of the (0–0) transitions of CN are perturbed by other electronic states, these levels are not taken into account for the temperature determination. The rotational–vibrational spectra of CN ($\Delta v = 0$) and CN ($\Delta v =$

−1) are calculated as a function of varying rotational and vibrational temperatures, and for an apparatus function evaluated to 0.25 Å, which was found experimentally.

Results

Before comparing experimental and calculated spectra to determine the rotational and vibrational temperatures, some observations must be taken into account. The observed bandhead of the (1−1) transition is lower than the calculated one for a given temperature when the other bandheads correspond well. The same observation holds for the transition (0−1). It can be assumed that the vibrational level $v = 1$ is not in equilibrium with the other vibrational levels. For the spectra because of the transitions $\Delta v = 0$, the best fit is performed for the (0−0), (2−2), and (3−3) bandheads. For the computation the molecular constants were taken from Herzberg,[14] which are valid for $v = 0$, 1, 2, and 3. Thus, for those spectra containing the transition $\Delta v = -1$, the bandheads (5−6), (4−5), and (3−4) cannot be used for the determination of the vibrational and rotational temperatures. Figure 11 presents the experimentally gained spectrum of the $\Delta v = 0$ band of CN at the nozzle exit, and Fig. 15 presents the calculated one that fit best. The vibrational and the rotational temperature could be determined to T_r = 4000 K and T_v = 8000 K by a comparison of Figs. 11 and 15.

At two axial generator positions (0 and 15 cm) the $\Delta v = -1$ band spectra of the CN molecule was recorded and analyzed by the comparing method additionally. The rotational and vibrational temperatures at the nozzle exit deduced with a precision of ±1000 K are similar to the temperatures that are found with the $\Delta v = 0$ band. Figures 12 and 16 depict the $\Delta v = -1$ band found experimentally and by simulation for T_v = 9000 K and T_r = 4500 K.

An axial temperature profile, range 0−45 cm, is obtained by analyzing the $\Delta v = 0$ band of CN, and is presented in Fig. 17. It can be observed that the vibrational temperature is higher than the rotational temperature along the axis. Taking into account the precision of the applied method (±500 K), the rotational temperature is constant between 0−45 cm, while the vibrational temperature rises slightly with increasing distance to the nozzle exit. An explanation for this behavior can be found by considering an expanding nonequilibrium flow.[15] Normally, it is assumed that the vibrational energies are contained in the electronic ground state and that molecules behave as a harmonic oscillator. In a nonequilibrium region, the upper states of the internal modes are generally underpopulated and attain number densities smaller than those given by the Boltzmann relations, which overestimate the internal energy.[16] Those overpopulated states contain energy that is not accounted for by the Boltzmann distribution, and so the temperatures calculated and presented in this article are overestimated far from the nozzle exit.

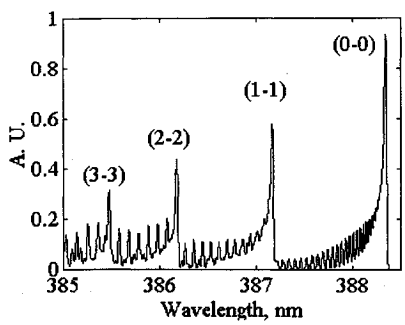

Fig. 15 $\Delta v = 0$ band structure of CN calculated for T_v = 8000 K and T_r = 4000 K.

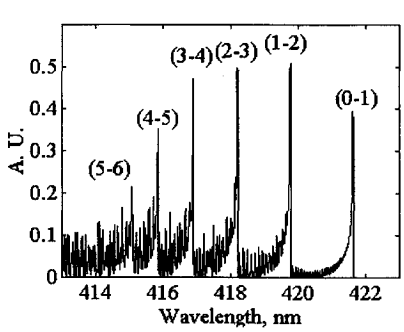

Fig. 16 $\Delta v = -1$ band structure of CN calculated for T_v = 9000 K and T_r = 4500 K.

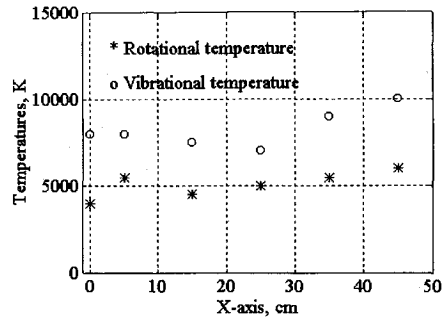

Fig. 17 Axial profile of the vibrational and rotational temperatures in an N_2−CH_4 plasma.

It is intended to enclose the Treanor[17] distribution in the simulation program of CN to calculate the vibrational population distribution and then to apply the new simulation to the $\Delta v = 0$ band of CN to determine the rotational and vibrational temperatures. Another behavior of the temperature profile can be expected other than that found with the Boltzmann population distribution.

The emission because of the transition $A^3\Pi \rightarrow X^3\Sigma$ of NH is observed along the axis (Fig. 13), and it is planned to determine the rotational temperature using the Boltzmann plot with an appropriate simulation program. The comparison of the temperatures deduced from the NH and CN molecules will give evidence for a thermal nonequilibrium between different electronic levels.

In the CO_2−N_2 plasma, the $\Delta v = 0$ band of the CN molecule is not well enough resolved to be analyzed. Figure 14 presents a spectrum recorded at the nozzle exit. The rotational structure is perturbed by the background noise and impurities, and so, unfortunately, no rotational and vibrational temperatures could be deduced. Other molecular emissions have been searched, such as N_2, C_2, and CO, but without success.

Discussion and Conclusions

The plasma environments occurring during the entry flights into the atmospheres of Titan and Mars have been simulated by 99% nitrogen and 1% methane, and 97% carbon dioxide and 3% nitrogen mixtures, respectively, and are investigated using mass spectrometry and emission spectroscopy.

A mass spectrometric survey along the central axis revealed the presence of a great variety of species, especially in the methane-containing flow. Rotational and vibrational temperatures were determined for the N_2−CH_4 case by analyzing the spectra of CN to be T_v = 9000 K and T_r = 5000 K at the nozzle exit. The most luminous species was found to be CN for both gas mixtures, even when the concentration is less than 1%. The predominant molecular species such as CO, O_2, O_2^+, for the CO_2−N_2 and N_2 for the N_2−CH_4 mixtures were obviously not excited electronically to emit radiation sufficient for the determination of temperatures. Unfortunately, the line spectra of atomic species such as N^+ or N, whose presence was detected through mass spectrometry, was not studied with the optical technique in this series of experiences.

For complete flow characterization, future investigation will concentrate on 1) numerical simulation of the NH band radi-

ation to obtain additional rotational and vibrational temperature information, 2) measurement of electron temperature and density, and 3) measurement of flow velocity by means of an electrostatic technique. Options are being examined for the possibility of the addition of a small amount of argon for both gas mixtures.

References

[1]Lago, V., Schönemann, A., Buuron, A., Lasgorceix, P., and Dudeck, M., "Supersonic Plasma Jets Device for Testing Space Craft Materials," 2nd European Symposium on Aerothermodynamics for Space Vehicles, ESTEC, Noordwijk, The Netherlands, Nov. 1994.

[2]Nelson, H. F., Park, C., and Whiting, E. E., "Titan Atmospheric Composition by Hypervelocity Shock-Layer Analysis," *Journal of Thermophysics and Heat Transfer*, Vol. 5, No. 2, 1991, pp. 157–165.

[3]Park, C., Howe, J. T., Laffe, R. L., and Candler, G. V., "Review of Chemical-Kinetics of Future NASA Missions, II: Mars Entries," *Journal of Thermophysics and Heat Transfer*, Vol. 8, No. 1, 1994, pp. 9–23.

[4]Lasgorceix, P., Lago, V., Asselin, P., and Dudeck, M., "Diagnostic Methods in an Air Plasma Jet at Low Pressure," 21st International Conf. on Phenomena in Ionized Gases, ICPIG, Bochum, Germany, 1993.

[5]Cernogora, G., Hochard, L., Dudeck, M., Lasgorceix, P., Lago, V., and Arepalli, S., "Optical Emission Spectroscopy of Air in a Rarefied Arc-Jet Flow," AIAA Paper 94-2426, June 1994.

[6]Peter, G., and Höfler, K., "Summary Abstract: Mass and Energy Analysis of Ions from Plasmas," *Journal of Vacuum Science Technology*, A, Vol. 5, No. 4, 1987, p. 2285.

[7]Schönemann, A., and Auweter-Kurtz, M., "Characterization of Nitrogen and Air Plasma Flows by Mass Spectrometry," 11th International Symposium on Plasma Chemistry, Loughborough, England, UK, 1993.

[8]Schönemann, A., Auweter-Kurtz, M., Habiger, H., Sleziona, C., and Stöckle, T., "Analysis of the Argon Additive Influence on a Nitrogen Arcjet Flow," *Journal of Thermophysics and Heat Transfer*, Vol. 8, No. 3, 1994, pp. 466–472.

[9]Schönemann, A., and Auweter-Kurtz, M., "Mass Spectrometric Investigation of High Enthalpy Plasma Flows," *Journal of Thermophysics and Heat Transfer*, Vol. 9, No. 4, 1995, pp. 620–628.

[10]Cernogora, G., Hochard, L., Dudeck, M., Lasgorceix, P., and Lago, V., "Vibrational Temperatures Measurements in Arc Jets," AIAA Paper 93-3229, July 1993.

[11]Koulidiati, J., "Etude Spectroscopique des Molécules Carbonées Diatomiques. Application au Diagnostic des Plasmas d'Hydrocarbures," Thesis, University of Orleáns, France, 1991.

[12]Huddlestone, R. H., and Leonard, S., *Plasma Diagnostic Techniques*, Academic, New York, 1965.

[13]Knowles, P., Werner, H.-J., Cartwright, D., and Hay, P., "The $X^2\Sigma \rightarrow B^2\Sigma$ Violet Systems of the CN Radical: Accurate Multireference Configuration Interactions of the Radiative Transition Probabilities," *Journal of Chemical Physics*, Vol. 89, No. 12, 1988, pp. 7334–7343.

[14]Herzberg, G., *Molecular Spectra and Molecular Structure*, Vol. III, Van Nostrand, New York, 1966.

[15]Park, C., "Estimation of Excitation Energy of Diatomic Molecules in Expanding Nonequilibrium Flows," *Journal of Thermophysics and Heat Transfer*, Vol. 9, No. 1, 1995, pp. 17–25.

[16]Park, C., *Nonequilibrium Hypersonic Aerothermodynamics*, Wiley, New York, 1990.

[17]Treanor, C. E., Rich, J. W., and Rehm, R. G., "Vibrational Relaxation of Anharmonic Oscillators with Exchange-Dominated Collisions," *Journal of Chemical Physics*, Vol. 48, No. 4, 1968, pp. 1798–1807.